NACA RM E54D06

RESEARCH MEMORANDUM

PUMPING AND DRAG CHARACTERISTICS OF AN AIRCRAFT EJECTOR AT SUBSONIC AND SUPERSONIC SPEEDS

By Gerald C. Gorton

Lewis Flight Propulsion Laboratory
Cleveland, Ohio

NATIONAL ADVISORY COMMITTEE
FOR AERONAUTICS

WASHINGTON

June 3, 1954

NACA RM E54D06

NATIONAL ADVISORY COMMITTEE FOR AERONAUTICS

RESEARCH MEMORANDUM

PUMPING AND DRAG CHARACTERISTICS OF AN AIRCRAFT EJECTOR AT SUBSONIC AND SUPERSONIC SPEEDS

By Gerald C. Gorton

SUMMARY

An investigation was conducted in the 8- by 6-foot supersonic wind tunnel on a cylindrical-shroud ejector (diameter ratio of 1.2 and spacing ratio of 0.80). Data were obtained at weight-flow ratios of 0.014, 0.095, 0.234, and 0.380 for primary pressure ratios ranging from 1 to 16 and at free-stream Mach numbers of 0.1, 0.6, 1.6, and 2.0.

The results of this investigation indicate no effect of free-stream Mach number on the pumping characteristics of an ejector of this type. Boattail pressure-drag and base pressure-drag coefficients were found to decrease with increasing primary pressure ratio similar to conventional nozzles. It was also found that these drag coefficients decreased as weight-flow ratio was increased.

The results also indicate that the primary-nozzle mass-flow coefficient was affected by the secondary flow. Apparently the internal geometry of the secondary passage, at the exit station of the primary nozzle, was critical in effecting a decrease in primary-nozzle mass-flow coefficient as weight-flow ratio was increased to values greater than 0.10.

INTRODUCTION

Considerable effort has been expended to evaluate ejector performance, but this work has been largely limited to quiescent-air investigations (e.g., ref. 1). Consideration must also be given to any possible effect free-stream Mach number might have on the internal performance of an ejector, inasmuch as ejectors may be used to satisfy the cooling and thrust requirements of aircraft operating over a wide range of flight speed. For a plug nozzle and a series of convergent-divergent nozzles, references 2 and 3 indicated that the internal performance was generally insensitive to external flow except for the condition of flow separation from the convergent-divergent nozzle wall. However, it is not evident, without investigation, that these results are applicable to an ejector nozzle.

In addition to the effect of free-stream Mach number on the pumping characteristics, information is lacking regarding the effect of the jet on the external characteristics, as was discussed in references 4 and 5 for fixed nozzles. In the case of the ejector, there is the added variable of weight-flow ratio which might also affect the amount of interaction between the internal and external flow.

The pumping and drag characteristics for a cylindrical-shroud ejector (diameter ratio of 1.2 and spacing ratio of 0.80) are evaluated for weight-flow ratios of 0.014, 0.095, 0.234, and 0.380 at free-stream Mach numbers of 0.1, 0.6, 1.6, and 2.0 for primary pressure ratios ranging from 1 to 16. The results are presented for zero angle of attack and for a primary jet temperature of 860° R. Limited data are also presented for an angle of attack of 8° and for primary jet temperatures ranging from 1500° to 2000° R.

This investigation was conducted at the NACA Lewis laboratory.

SYMBOLS

The following symbols are used in this report:

A_{max}	maximum model cross-sectional area, 0.371 sq ft
C_D	coefficient of drag, $F/q_O A_{max}$
C_P	coefficient of pressure, $(p_x-p_O)/q_O$
D	diameter, ft
D_s/D_p	diameter ratio
F	drag force, lb
f	fuel flow, lb/sec
L	length of shroud from primary-nozzle exit, ft
L/D_p	spacing ratio
M	Mach number
P	total pressure, lb/sq ft
p	static pressure, lb/sq ft
q	dynamic pressure, lb/sq ft

T	total temperature, $^{\circ}R$
U	total air flow, lb/sec
W	weight flow, lb/sec
$\frac{W_s}{W_p}\sqrt{\frac{T_s}{T_p}}$	weight-flow ratio
α	angle of attack, deg
γ	ratio of specific heats

Subscripts:

a	boattail
b	base
e	effective
i	ideal
p	primary nozzle
s	secondary nozzle
t	total
x	axial distance
0	free stream

APPARATUS AND PROCEDURE

The generalized exit model with an ejector afterbody was installed in the 8- by 6-foot supersonic wind tunnel as schematically illustrated in figure 1 (see ref. 2 for details). Air was directed into the model by means of two hollow support struts. This air was preheated to a temperature of approximately 860° R in order to eliminate possible condensation effects within the nozzle. A limited amount of data was obtained for ejector primary-air temperatures ranging from 1500° to 2000° R by using a can-type gasoline combustor (fig. 2) located ahead of the primary nozzle.

The geometric characteristics of the ejector, including static-pressure instrumentation, are shown in figure 2. Secondary flow was bled from the primary chamber through six equally spaced ports located around the circumference at station 3. A rotatable metal ring which enclosed various portions of the bleed ports made it possible to control the secondary flow.

An A.S.M.E. sharp-edged orifice, located upstream of the model, was used to measure the total air flow U through the model, whereas the fuel flow f to the preheater and the main combustor was measured by independent rotameters. The secondary weight flow W_s was determined from a calibration of the bleed-port mechanism used in conjunction with pressure measurements across the port. Primary weight flow W_p was calculated by a summation of the total air flow, fuel flow, and secondary weight flow as follows:

$$W_p = U + f - W_s \tag{1}$$

The total pressures in the primary and secondary nozzles were obtained from continuity relations, with the total temperature, weight flow, and static pressure of the respective streams known at a given station. Primary-nozzle total pressure was calculated at station 6, whereas the secondary-nozzle total pressure was determined at station 4. For the case of hot flow (1500° to 2000° R), the primary-nozzle mass-flow coefficient was assumed to be the same as for the equivalent cold-flow case (860° R). The primary total pressure and jet temperature could then be computed.

Mass-flow coefficients for the primary nozzle, with cold flow, were calculated as the ratio of computed primary weight flow W_p, to the ideal primary weight-flow $W_{p,i}$ which was determined from continuity relations for a choked nozzle, with the total temperature, total pressure, and geometric area known at the primary-nozzle exit.

Boattail pressure drag was obtained from an integration of the static pressures measured along the boattail. Static-pressure orifices on the top and bottom of the boattail were located axially as indicated in figure 2. The base pressure drag was calculated from the static pressures measured at the base of the ejector. These static pressures were measured by three orifices, located one each on the top, bottom, and a side.

In order to arrive at a total-drag value for the configuration, a value of nose pressure and friction drag, taken from reference 4 for the same basic model, was used in conjunction with the values of boattail pressure drag and base pressure drag of the investigation reported herein.

RESULTS AND DISCUSSION

Internal Characteristics

Pumping characteristics of the ejector are presented in figure 3. These data, which were obtained for primary pressure ratios ranging from 1 to 16, show no effect of free-stream Mach number or angle of attack on the pumping characteristics. It therefore seems reasonable to assume that the thrust characteristics of such an ejector would likewise be unaffected.

Mass-flow coefficients for the primary nozzle are unaffected by free-stream Mach number or primary pressure ratio, as indicated in figure 4(a). However, there appears to be a change in mass-flow coefficient with weight-flow ratio (fig. 4(b)). The mass-flow coefficient is maintained constant at 0.95 to weight-flow ratios of approximately 0.10, but decreases with increasing weight-flow ratio until at a weight-flow ratio of 0.380 the mass-flow coefficient has decreased to 0.85, indicating the formation of a vena contracta downstream of the primary-nozzle-exit station.

In correlating the pumping characteristics of this ejector with one of nearly equivalent diameter and spacing ratio investigated in quiescent air (ref. 1), it was found that only at the low weight-flow ratios (below 0.10), where the mass-flow coefficient of the present investigation was approximately the same as that of reference 1, was there reasonable agreement. To achieve better correlation at the larger weight-flow ratios, it was reasoned that a reduction in the mass-flow coefficient was equivalent to an increase in the ejector diameter ratio; therefore, an effective diameter ratio $(D_s/D_p)_e$ was assumed. The effective diameter ratio was obtained by replacing the geometric diameter of the primary nozzle with an effective diameter. Since the mass-flow through a nozzle varies as the square of the nozzle diameter, the effective diameter of the primary nozzle is defined as the geometric diameter multiplied by the square root of the mass-flow coefficient. Inasmuch as data were not available in reference 1 for ejectors of comparable effective diameter ratios, a linear interpolation at a constant primary pressure ratio was utilized, whereby pumping characteristics for geometric diameter ratios of 1.21 and 1.41, with respective spacing ratios of 0.796 and 0.855, covered the necessary range. The diameter ratios of reference 1 were also modified by their mass-flow coefficient (0.985) prior to interpolation.

The comparison in figure 5 showed generally good correlation, indicating that the effective diameter ratio is more significant than the geometric diameter ratio in predicting ejector pumping characteristics.

The essential difference between the ejector of reference 1, which had a geometric diameter ratio of 1.21 and a spacing ratio of 0.796, and the ejector reported herein is the geometry and flow direction of the secondary passage at the exit station of the primary nozzle (see illustration in fig. 5). The results of this investigation, therefore, indicate that the geometry of the secondary passage, as well as the spacing and diameter ratios, can influence the pumping characteristics of an ejector.

External Characteristics

Boattail pressure-drag coefficients, obtained by integrating the boattail pressure distributions (fig. 6, e.g.) are presented in figure 7 as a function of primary pressure ratio and weight-flow ratio. As would be expected, the boattail pressure drag of the ejector decreased as the primary-pressure ratio was increased. In addition to this overpressure effect of the jet, which is similar to that noted for conventional nozzles (ref. 4), there is also a reduction in boattail pressure drag with increased weight-flow ratio, probably as a result of the higher secondary total pressures present with increased weight-flow ratios.

Base pressure-drag coefficients were calculated from static-pressure measurements taken at the base of the ejector shroud and are presented in figure 8 as a function of primary pressure ratio and weight-flow ratio. As was observed with boattail pressure drag, the base pressure drag was decreased by the overpressure effect of the jet at the higher primary pressure ratios and by the higher secondary total pressures associated with an increase in weight-flow ratio.

Boattail pressure-drag, base pressure-drag, and total-drag coefficients are summarized in figure 9 as functions of primary pressure ratio and free-stream Mach number. Boattail pressure-drag coefficients are highest at $M_0 = 1.6$ for most of the primary pressure-ratio range and lowest at $M_0 = 0.6$. The greatest change with primary pressure ratio was noted at $M_0 = 1.6$, similar to the results of references 4 and 5. Base pressure-drag coefficients increase with free-stream Mach number at a constant primary pressure ratio and are affected by the primary pressure ratio in a similar manner at each Mach number. The total-drag coefficients presented are a summation of the boattail pressure-drag and base pressure-drag coefficients plus a coefficient of nose pressure and friction drag taken from reference 4 for the same basic model. Such a summation indicates the relative significance of boattail pressure drag and base pressure drag as components of total drag. For this configuration, the base drag was relatively insignificant to the total drag, since the base was merely the thickness of the metal at the base of the shroud.

A limited amount of hot-flow drag data is included in figure 9 for comparison with the drag data obtained with cold flow for the same bleed-port setting (weight-flow ratio of 0.014). These data for $M_0 = 1.6$ and 2.0 indicated a very slight decrease in boattail pressure drag with an increase in temperature. This trend is supported by observations made from schlieren photographs and static-pressure distributions which indicate an upstream movement of the trailing shock, which was also noted in reference 6.

SUMMARY OF RESULTS

The following results were obtained from an investigation in the 8- by 6-foot supersonic wind tunnel of a cylindrical-shroud ejector (diameter ratio of 1.2 and spacing ratio of 0.8). The data were obtained for weight-flow ratios of 0.014, 0.095, 0.234, and 0.380 for primary pressure ratios ranging from 1 to 16 and at free-stream Mach numbers of 0.1, 0.6, 1.6, and 2.0.

1. There was no apparent effect of free-stream Mach number or angle of attack on the pumping characteristics of the ejector investigated.

2. Boattail pressure-drag and base pressure-drag coefficients decreased with increasing primary pressure ratio similar to conventional nozzles. In addition, these drag coefficients decreased with increasing weight-flow ratio.

3. The primary-nozzle mass-flow coefficient decreased considerably as the weight-flow ratio was increased to values greater than 0.10. Apparently the internal geometry of the secondary passage at the exit station of the primary nozzle is critical in establishing this trend with weight-flow ratio.

Lewis Flight Propulsion Laboratory
National Advisory Committee for Aeronautics
Cleveland, Ohio, March 31, 1954

REFERENCES

1. Greathouse, W. K., and Hollister, D. P.: Air-Flow and Thrust Characteristics of Several Cylindrical Cooling-Air Ejectors with a Primary to Secondary Temperature Ratio of 1.0. NACA RM E52L24, 1953.

2. Hearth, Donald P., and Gorton, Gerald C.: Investigation of Thrust and Drag Characteristics of a Plug-Type Exhaust Nozzle. NACA RM E53L16, 1954.

[redacted]

3. Fradenburgh, Evan A., Gorton, Gerald C., and Beke, Andrew: Thrust Characteristics of Series of Convergent-Divergent Exhaust Nozzles at Subsonic and Supersonic Flight Speeds. NACA RM E53L23, 1954.

4. Englert, Gerald W., Vargo, Donald J., and Cubbison, Robert W.: Effect of Jet-Nozzle-Expansion Ratio on Drag of Parabolic Afterbodies. NACA RM E54B12, 1954.

5. Vargo, Donald J., and Englert, Gerald W.: Effect of Nozzle Contour on Drag of Parabolic Afterbodies. NACA RM E54D02, 1954

6. Hearth, Donald P., and Wilcox, Fred A.: Thrust and Drag Characteristics of a Convergent-Divergent Nozzle with Various Exhaust Jet Temperatures. NACA RM E53L23b, 1954.

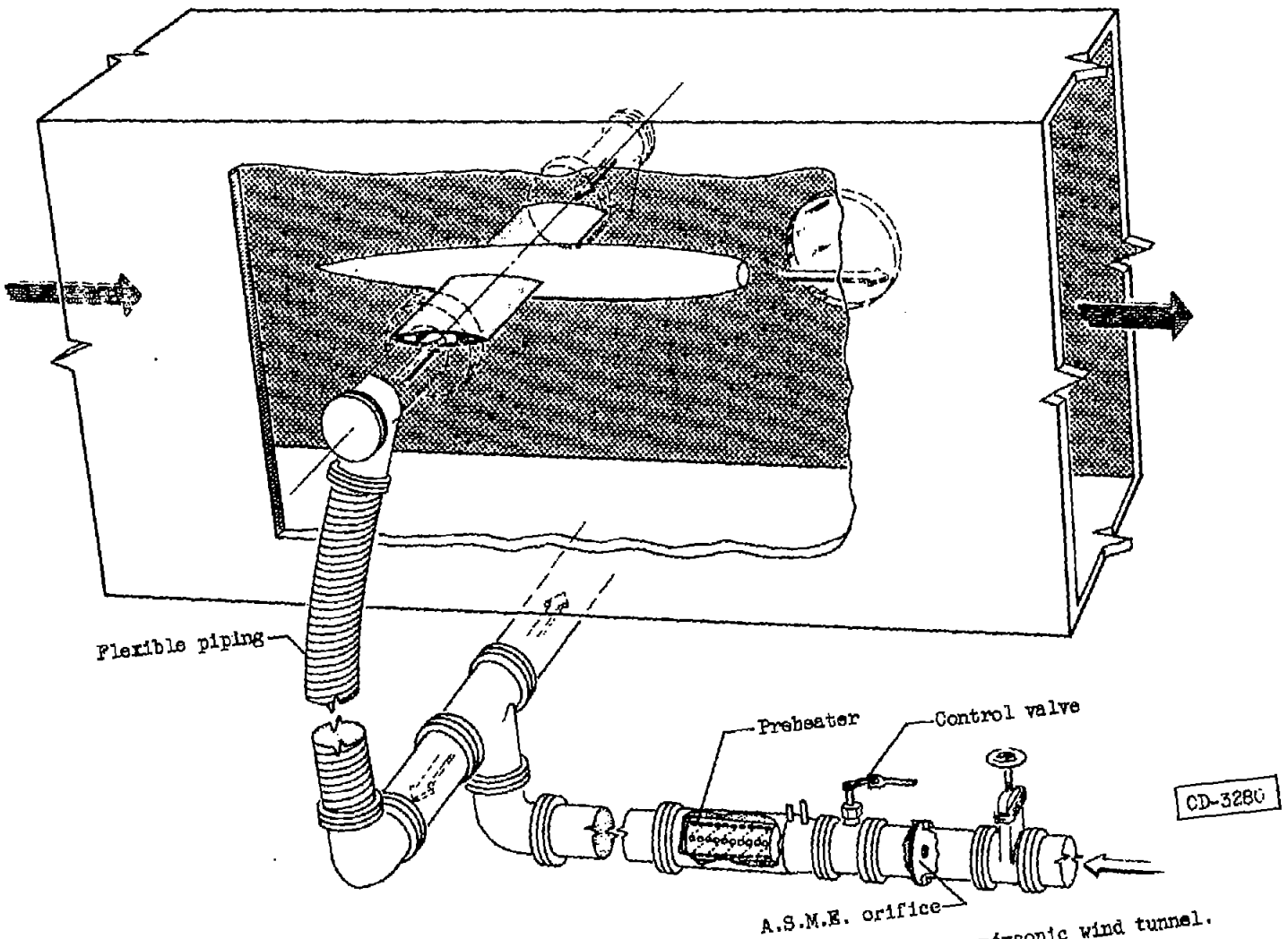

Figure 1. - Schematic diagram of jet-exit model installed in 8- by 6-foot supersonic wind tunnel.

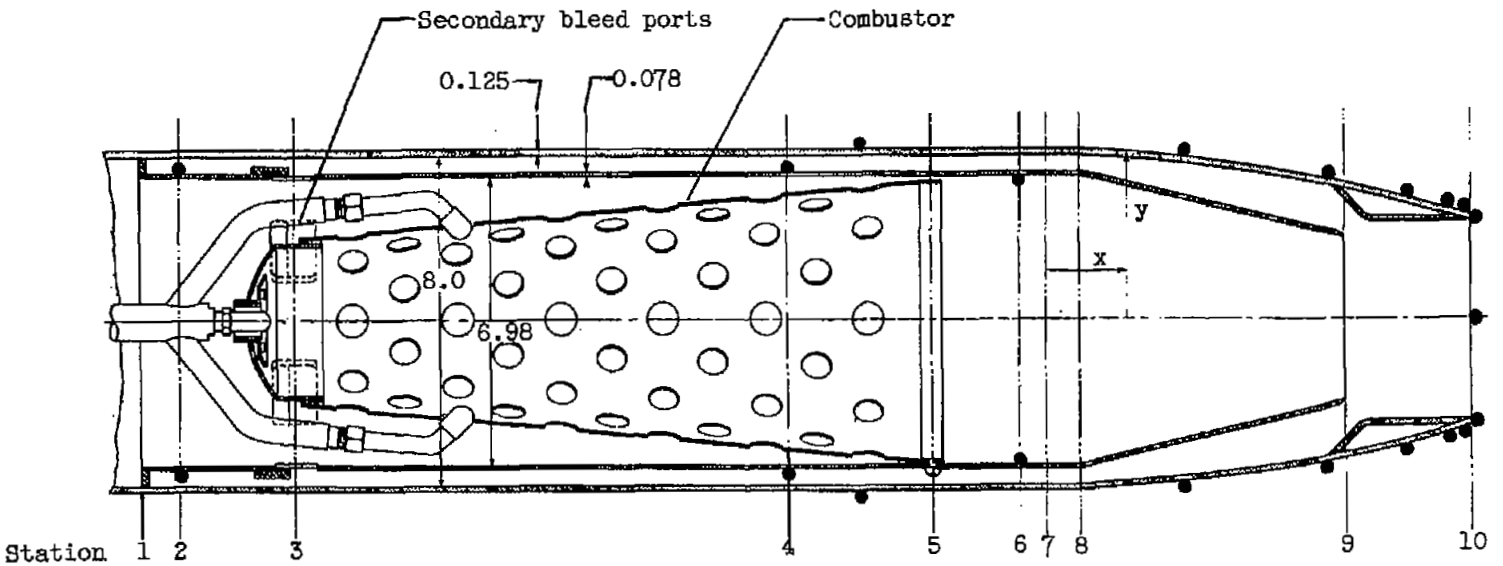

Equation of boattail: $y = 4.125\left[1 - \left(\frac{x}{18}\right)^2\right]$

Station	Axial distance from model nose
1	50.25
2	51.25
3	53.25
4	66.00
5	69.75
6	72.00
7	72.65
8	73.58
9	80.50
10	83.75

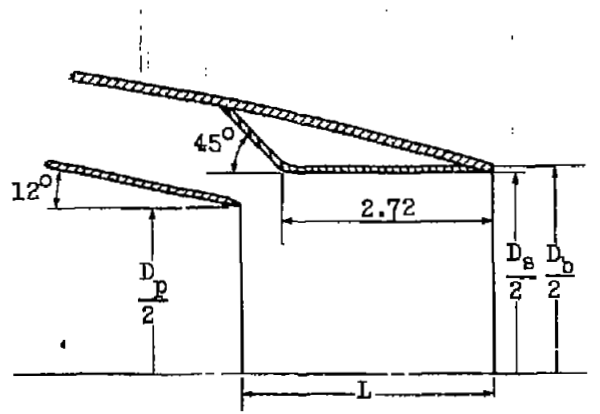

CD-3507

Static-pressure orifices

Figure 2. - Geometric characteristics of ejector configuration including static-pressure instrumentation. Diameter ratio, 1.2; spacing ratio, 0.8; base diameter ratio, D_b/D_s, 1.05. (All dimensions in inches.)

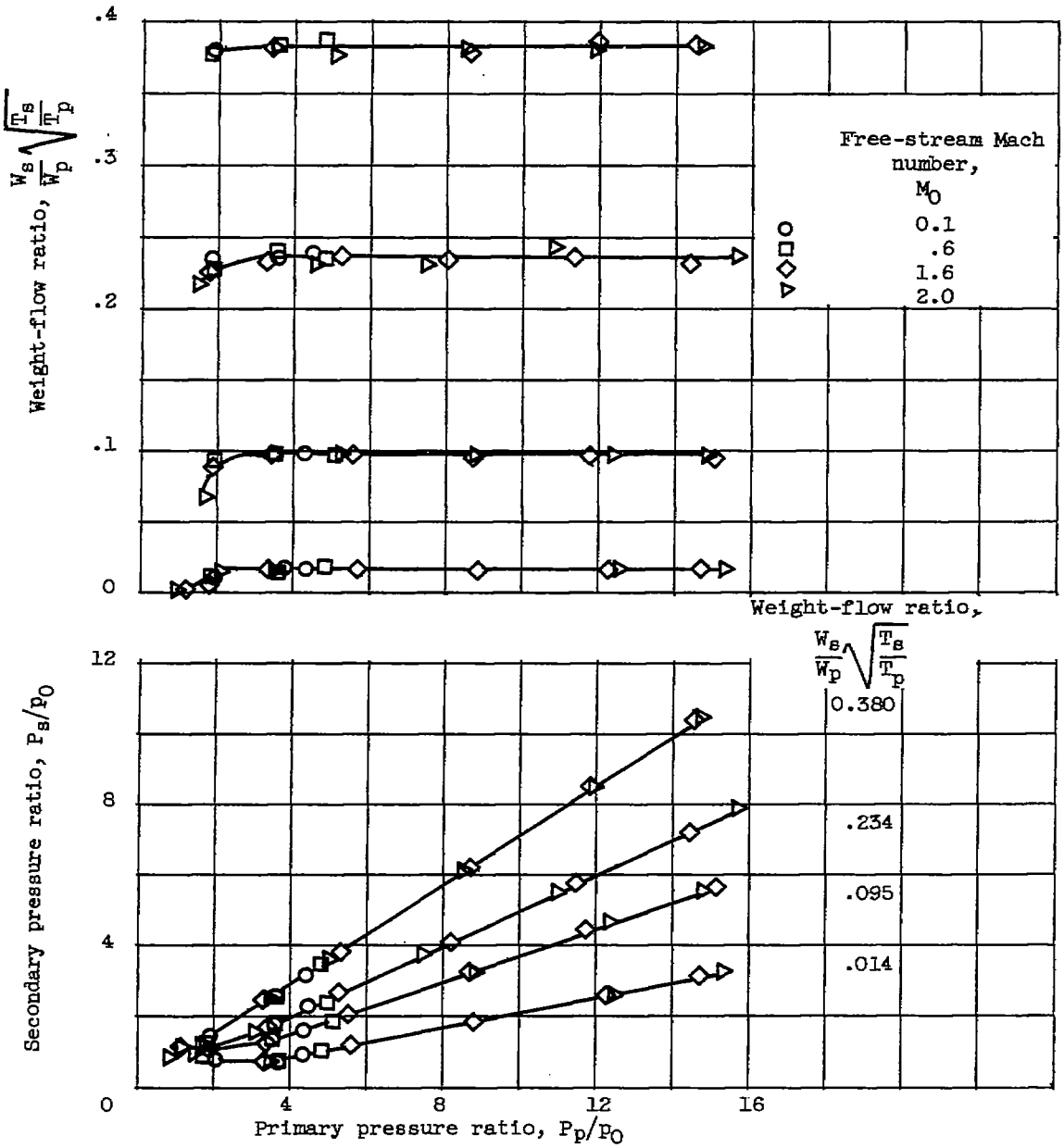

(a) Zero angle of attack.

Figure 3. - Pumping characteristics of ejector. Diameter ratio, 1.2; spacing ratio, 0.8.

[redacted]

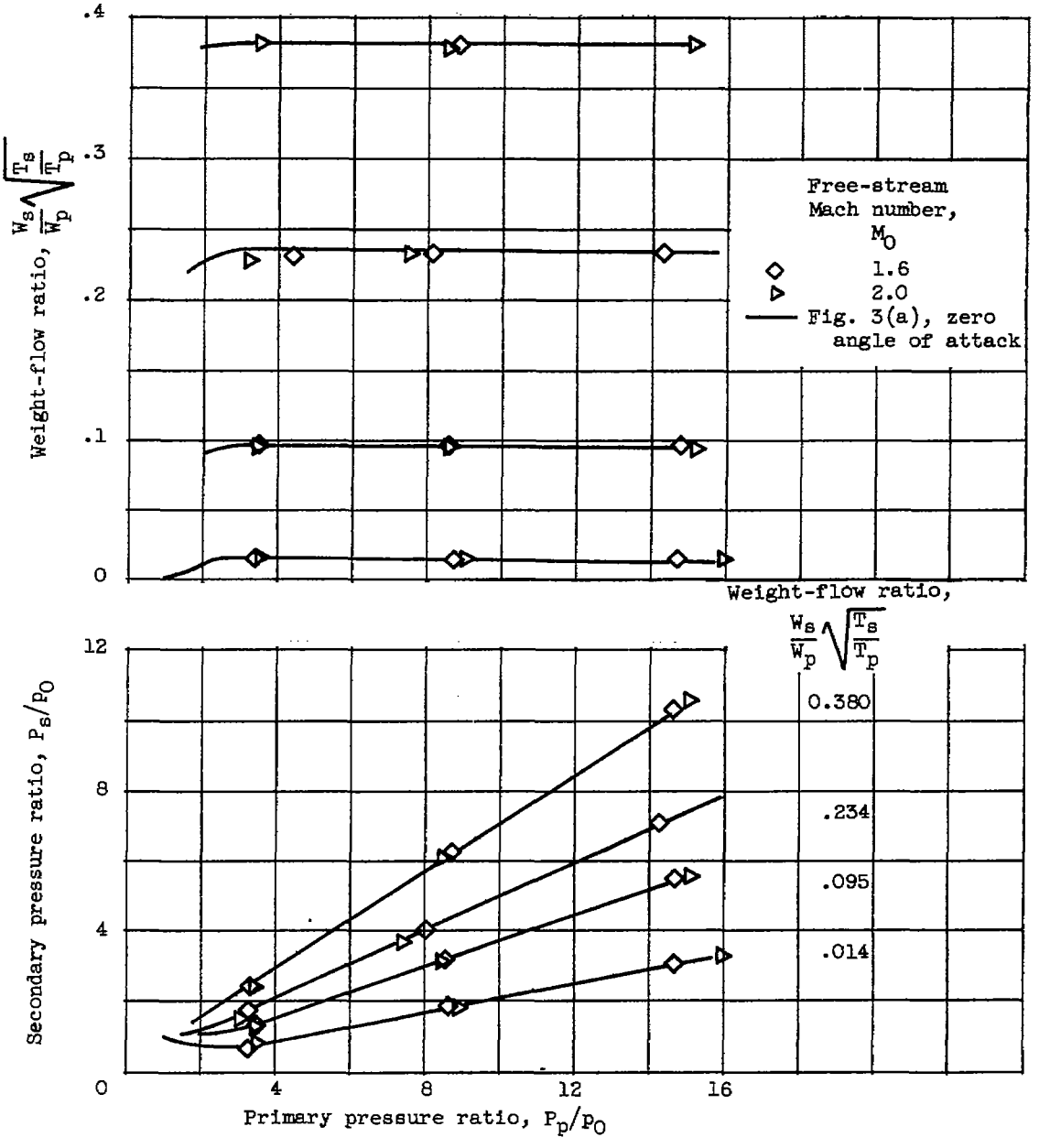

(b) Angle of attack, 8°.

Figure 3. - Concluded. Pumping characteristics of ejector. Diameter ratio, 1.2; spacing ratio, 0.8.

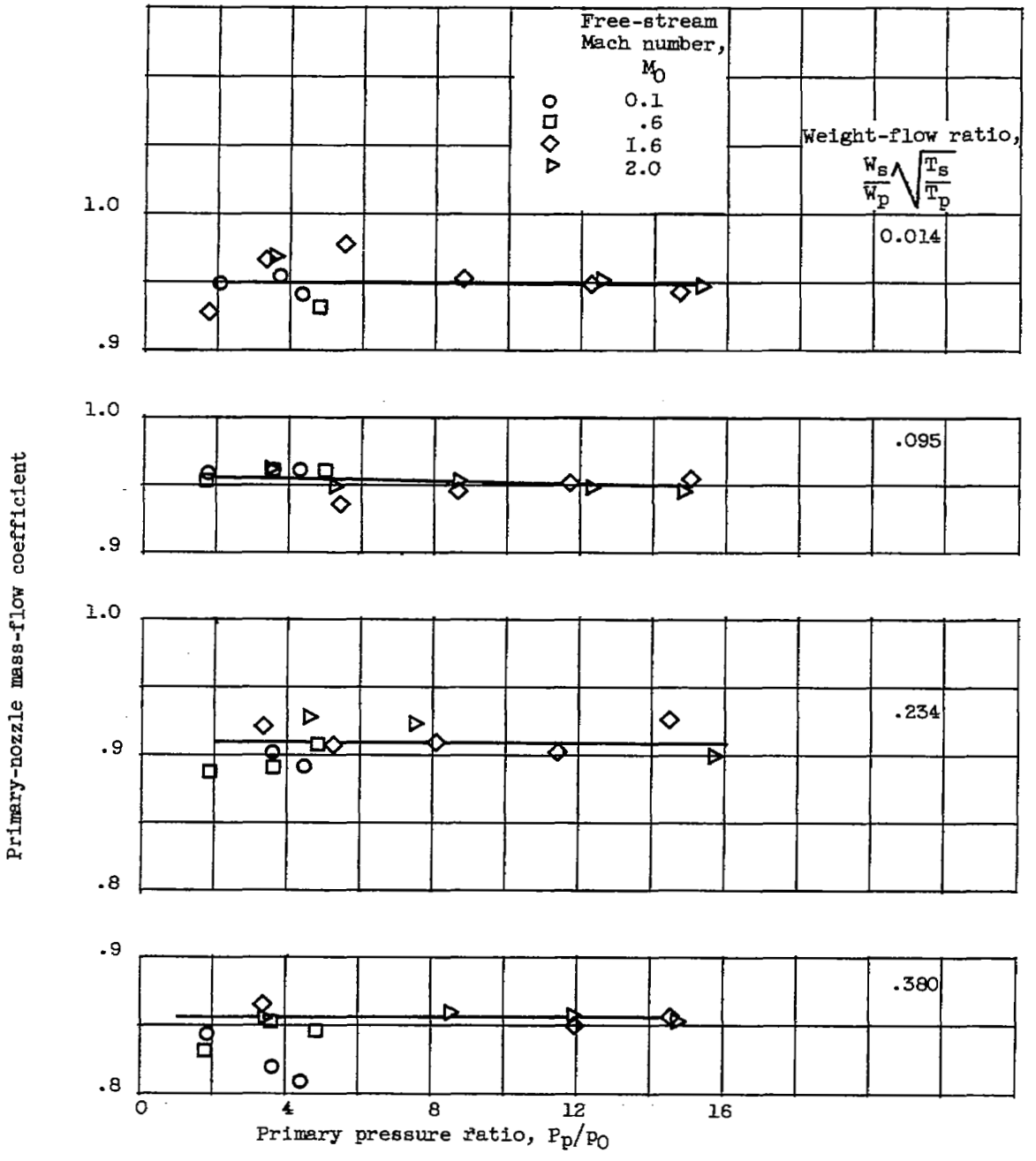

(a) Effect of primary pressure ratio and free-stream Mach number.

Figure 4. - Primary-nozzle mass-flow coefficients at zero angle of attack.

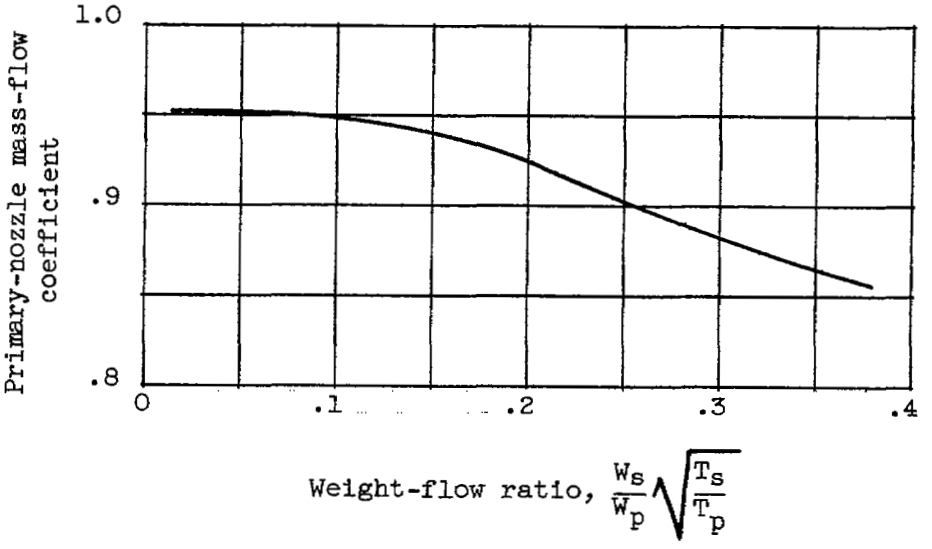

(b) Effect of weight-flow ratio.

Figure 4. - Concluded. Primary-nozzle mass-flow coefficients at zero angle of attack.

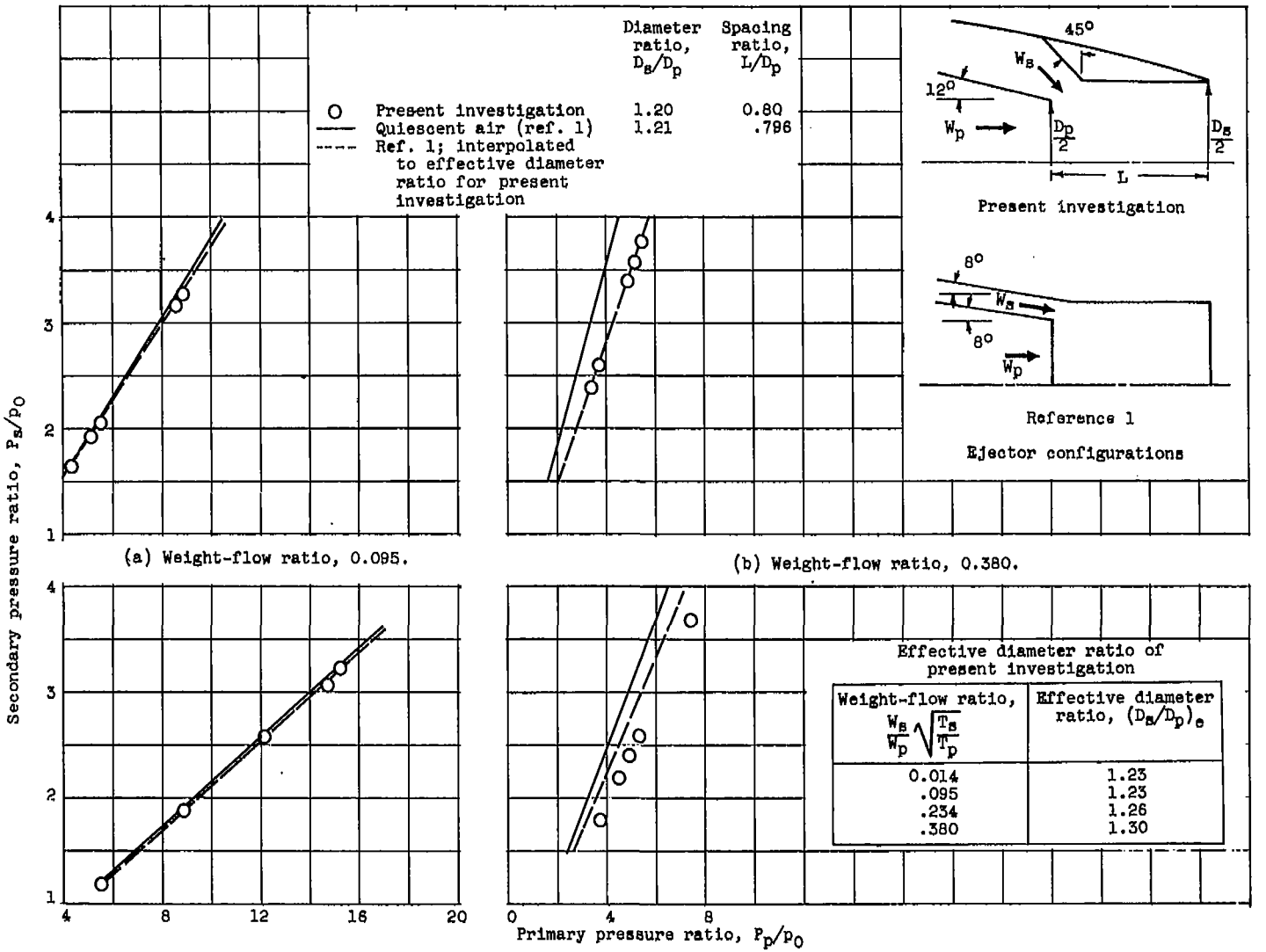

Effective diameter ratio of present investigation

Weight-flow ratio, $\frac{W_s}{W_p}\sqrt{\frac{T_s}{T_p}}$	Effective diameter ratio, $(D_s/D_p)_e$
0.014	1.23
.095	1.23
.234	1.26
.380	1.30

Figure 5. - Correlation of ejector pumping characteristics by use of effective diameter ratio.

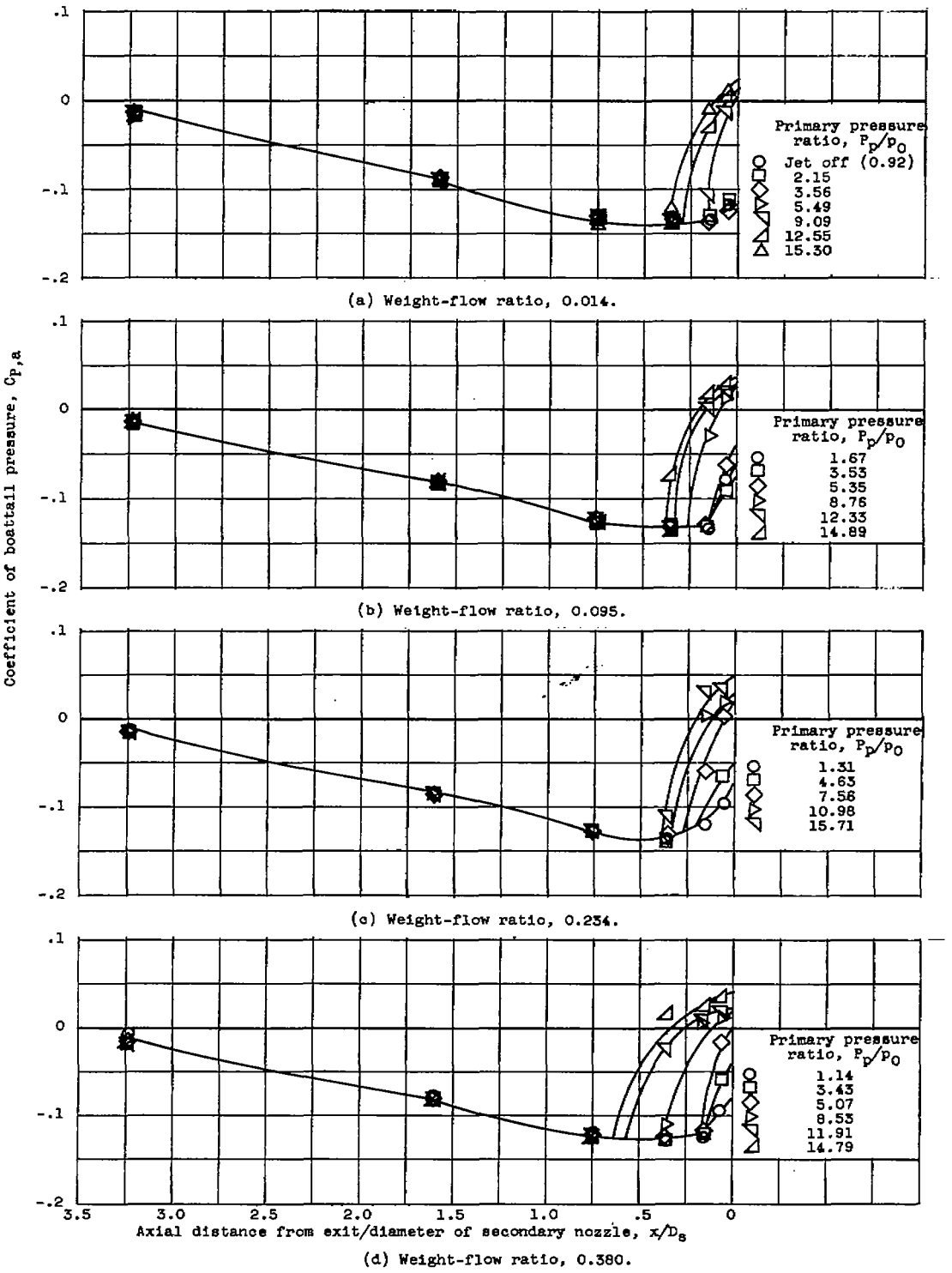

Figure 6. - Boattail pressure distributions at free-stream Mach number of 2.0 and zero angle of attack.

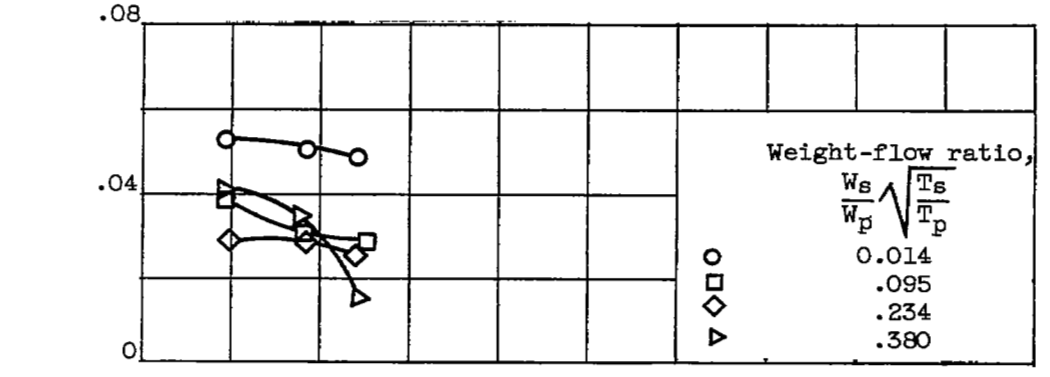

(a) Free-stream Mach number, 0.6.

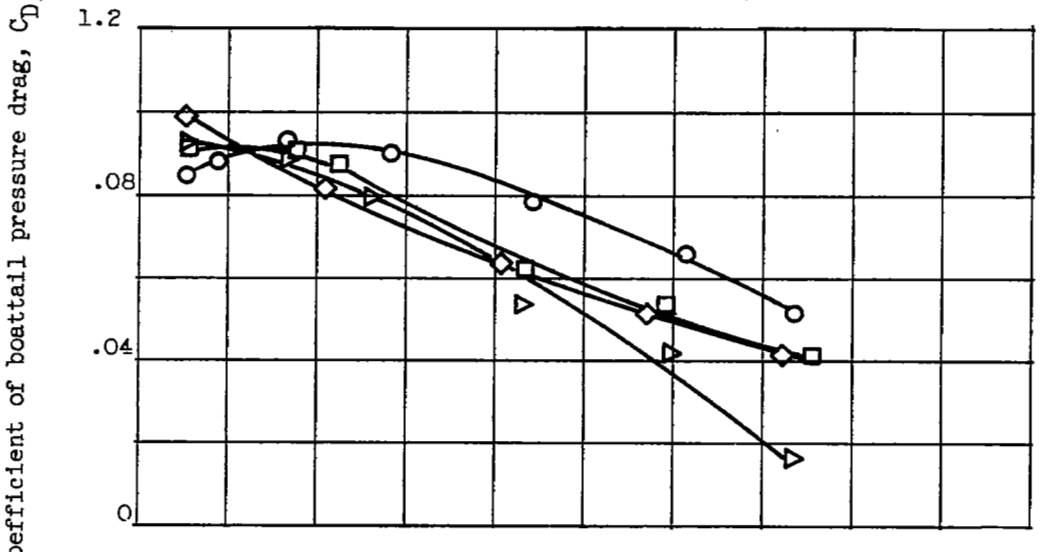

(b) Free-stream Mach number, 1.6.

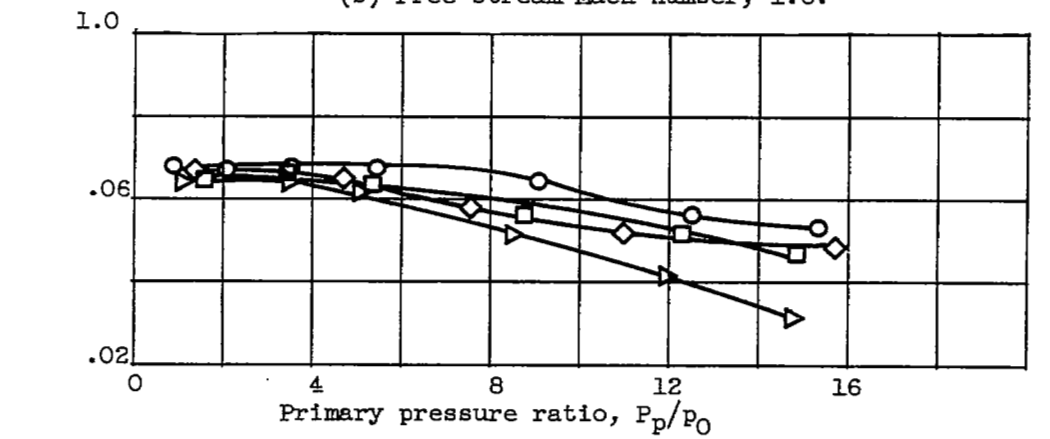

(c) Free-stream Mach number, 2.0.

Figure 7. - Boattail-pressure drag at zero angle of attack.

[redacted]

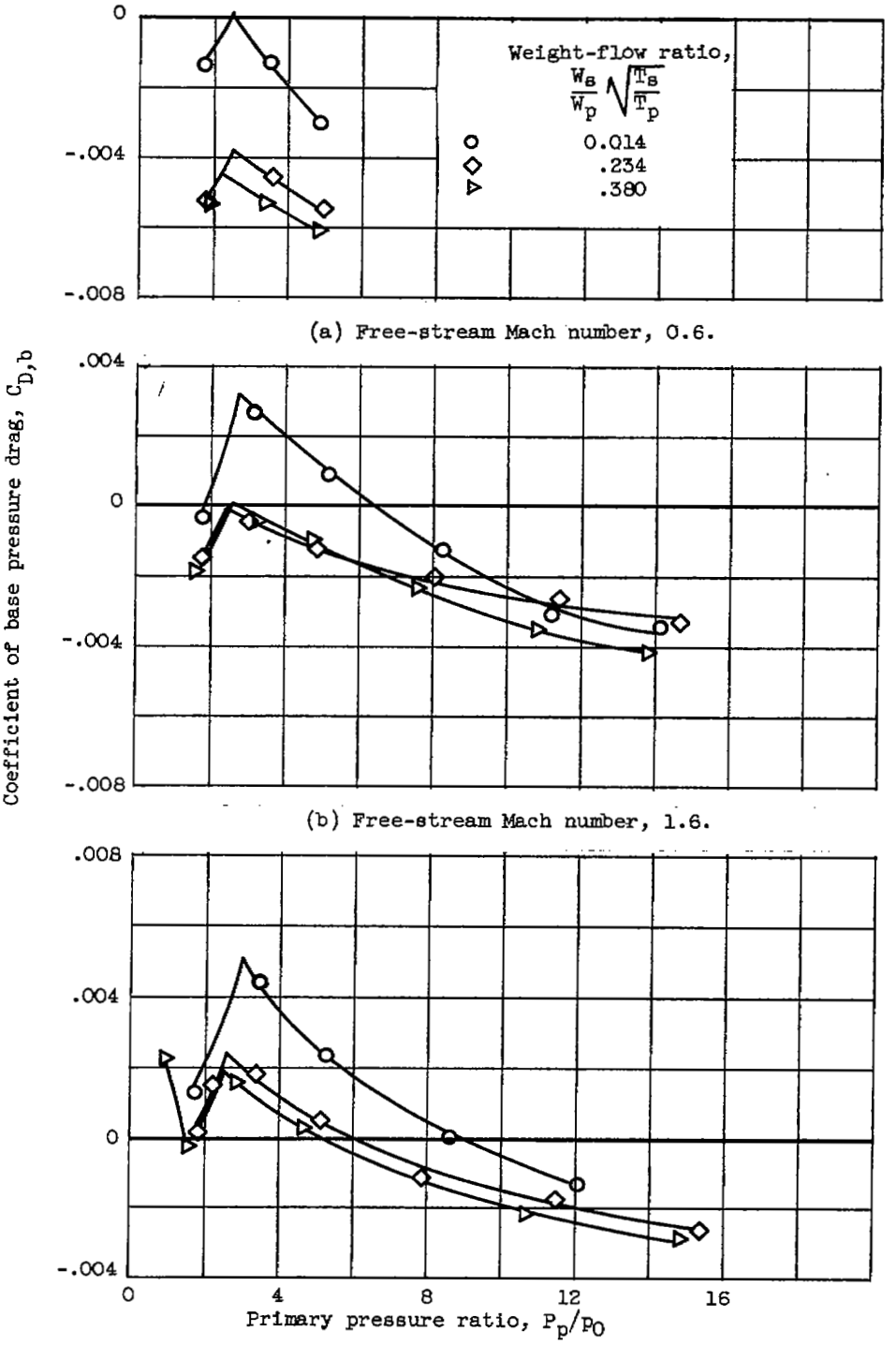

(a) Free-stream Mach number, 0.6.

(b) Free-stream Mach number, 1.6.

(c) Free-stream Mach number, 2.0.

Figure 8. - Base pressure drag at zero angle of attack.

[redacted]

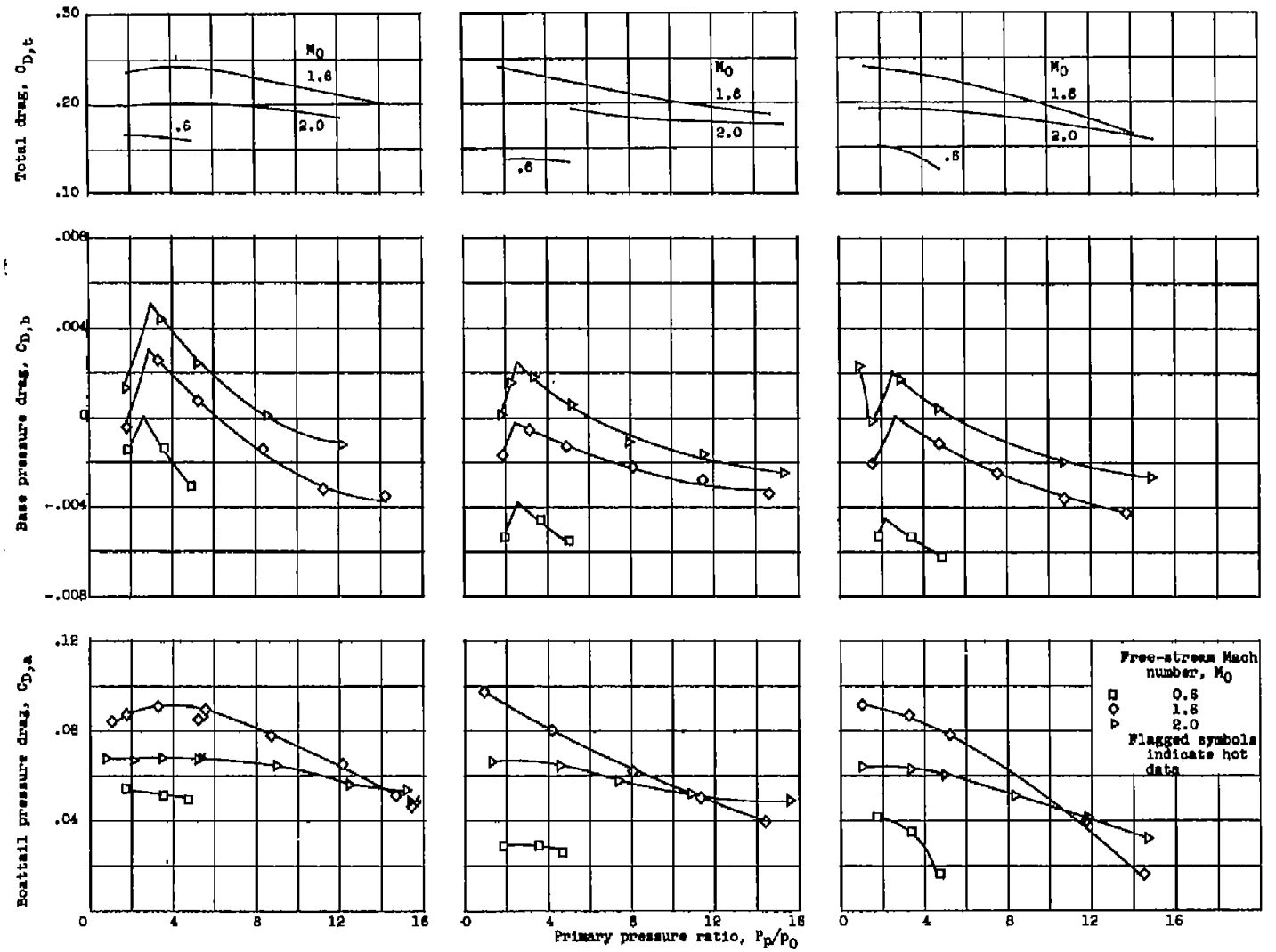

(a) Weight-flow ratio, 0.014. (b) Weight-flow ratio, 0.254. (c) Weight-flow ratio, 0.380.

Figure 9. - Coefficients of boattail pressure, base pressure, and total drag at zero angle of attack.